Effects of pH and Chloride Concentration on Corrosion Behavior of Duplex Stainless Steel and Titanium Alloys Ti 6Al 2Nb 1Ta 1Mo at Elevated Temperature for Pump Impeller Applications

Aymen A. Ahmed[†], Ammar Yaseen Burjes, and Marwan Zuhair Elias

Sciences College, Mosul University, Mosul, Iraq
(Received June 24, 2022; Revised August 11, 2022; Accepted September 07, 2022)

The objective of this study was to determine effects of temperatures and pH of sodium chloride solution with $MgCl_2$ ions on corrosion resistance of duplex stainless-steel X2CrNiMoN22-5-3 (DSS) and Ti 6Al 2Nb1Ta1Mo (Ti). Effects of sodium chloride concentration on corrosion resistance were also studied. Corrosion behavior and pitting morphology of duplex stainless steel (DSS) and Ti alloys were evaluated through potentiodynamic polarization, electrochemical impedance spectroscopy (EIS), and scanning electron microscopy (SEM). It was found that a decrease in pH significantly reduced the corrosion resistance of both alloys. Changes in chloride concentration and temperature had more substantial impact on corrosion behavior of DSS than on Ti alloys. Pitting corrosion was formed on DSS samples under all conditions, whereas crevice corrosion was developed on Ti samples with the presence of magnesium chloride at 90 °C. In conclusion, magnesium chloride ions in an exceedingly strong acidity solution appear to interact with re-passivation process at the surface of these alloys and influence the resulting surface topography.

Keywords: Corrosion, Duplex stainless steel, Titanium

1. Introduction

Deciding on construction materials is an essential component to the success of any pump application, and their initial cost is typically the primary consideration. Other factors to be considered in choosing these materials for moistened pump parts are users' experience, expected pump life, intermittent or continuous operation, pumping of hazardous or toxic liquids, fluid condition, pump suction power level, and service conditions [1].

Still, corrosion is the main problem leading to pumps, rapid failure, especially in harsh environments. The accelerated corrosion flux describes the removal of the protective oxide layer from the metal. The oxygen content, the flow velocity, and the chloride content are the most factors that accelerate this process. The effect of oxygen can be shown in the following example: Water with an oxygen content of fewer than 20 ppb (parts per billion) and a flow velocity of about 15 m/s will typically exhibit a corrosion rate of about 0.01 mm/year. However, increased oxygen content can increase the corrosion rate

to several mm/year, which will present a significant challenge to the process [2]. Some applications in the industry require centrifugal pumps to operate in fluid containing many solid particles and dissolved species at relatively high temperatures [3].

Stress corrosion and corrosion fatigue are two widespread forms of compressor impeller failure. Normally, serious uniform corrosion impeller failures can be avoided by choosing appropriate materials. Lowering the risk of failure due to corrosion makes it necessary to use high-quality materials such as titanium alloys because of their excellent strength and corrosion resistance. It shows exceptional resistance to a wide range of acids, alkalis, natural water, and industrial chemicals [4,5].

The differentiation in choosing titanium alloys may be governed by alloy elements and the environment in which the alloy works. Yue et al. [6] found that the Ti-6Al-4V alloy showed poor corrosion behavior in a solution with a high Cl⁻ concentration or acid environments with a local accumulation of Cl⁻ ions. Blanco-Pinzon et al. [7] reported that the Ti-6Al-4V alloy was prone to corrosion in H2SO4 solution, but its

corrosion resistance could be significantly affected by alloying Mo and Ni. The addition of Nickel accelerated the cathodic reactions while the addition of Mo retarded the anodic process [8]. Newman et al. [9] found that Molybdenum existing at defect sites preferentially dissolved, leading to the formation of stable Mo oxides to reduce the anodic dissolution rate [10]. Generally, alloying effectively improves the mechanical and corrosion properties of titanium and its alloys [11,12].

On the other hand, the most common stainless steel alloy submersible pumps have lower pH and chloride level ranges. Stainless steels are more prone to stress corrosion cracking in harsh environments. These factors lead to reduced pump life, higher servicing costs, and downtime- related revenue losses.

The Pitting Resistance Equivalency Number (PREN) is an acceptable measure of an alloy's suitability for seawater service, with PREN of 40 being the minimum generally accepted corrosion resistance. Only duplex stainless steels, exotic nickel alloys — including cupronickel can be the peer for titanium, especially if we consider the low cost compared to titanium alloys. Duplex (austenitic-ferritic) stainless-steels are very common in the oil and gas industries built after the 1970s. This expansion is associated with their good combination of properties, such as higher strength than austenitic stainless steel, better stress corrosion resistance, and similar price to traditional stainless-steels [13]. The duplex stainless steels differ mainly in chromium, nickel, and molybdenum contents compared to austenitic stainless steels. Chromium is a ferrite former. At higher chromium content, further nickel is necessary to form an austenitic or duplex structure. Higher chromium also boosts the formation of intermetallic phases. Typically there is at least 18% Cr in austenitic stainless steels and at least 22% in second-generation duplex stainless steels. The two-phase microstructure warranties higher resistance to pitting and stress corrosion cracking than conventional stainless steels [14].

With the aging of these structures, quantifying all factors contributing to the failure became more important. Two of those factors are chloride and the pH effects. These two factors are essential components of a failure analysis tool since many of the failures related to environments are linked to corrosion. Understanding the effect of the pH and the chloride concentration's effect is crucial in life assessment and the failure analysis of structures utilizing these alloys.

Like in other metals, corrosion in titanium and duplex stainless steel alloys breaks the basic properties due to chemical reactions with their surroundings. Specific environments offer opportunities for these metals to combine chemically with elements to form compounds and return to their lower energy levels. Ultimately, they corrode through contact with solutions like water (and moisture in the air), acids, bases, salts, oils, aggressive metal polishes, and other solid and liquid chemicals. They can also corrode when exposed to gaseous materials like acid vapors, formaldehyde gas, ammonia gas, and sulfur-containing gases.

The novelty of the current work is represented in the all details of the test that are of interest to the industrial sector and which is a decisive factor in choosing the appropriate alloys in the design of devices operating in various corrosion conditions. The economic factor is considered one of the most important, especially if take into account the high cost of some alloys such as titanium, which can be compensated for by less expensive alloys with the same efficiency in some operating conditions. The conditions related to corrosion are numerous, and each alloy needs to be scrutinized to know its capabilities under these conditions to resist corrosion.

The environment in which these alloys operate in many industrial applications, such as fluctuations in concentrations, differences in pH, and relatively high temperatures, calls us to test these materials in different environmental variables.

This study aims to cover several complicated environmental variables, including the effect of chloride concentration, pH, and temperature on the duplex stainless-steel and titanium alloys Ti 6Al 2Nb 1Ta 1Mo, to give us more accurate perceptions about the differentiation between these alloys and their use in the pump impeller applications.

2. Experimental procedure

2.1 Preparation of samples and solutions

Duplex austenitic stainless steel X2CrNiMoN22-5-3 (DSS) and Ti 6Al 2Nb 1Ta 1Mo (Ti) alloys were

AYMEN A. AHMED, AMMAR YASEEN BURJES, AND MARWAN ZUHAIR ELIAS

Table 1. Chemical composition of the X2CrNiMoN22-5-3 steel (DSS)

DSS	C	Si	Mn	P	N	Cr	Mo	Ni	Cu	Fe
wt%	0.024	0.41	1.39	0.027	0.16	22.15	2.56	5.98	0.13	bal.

Table 2. Chemical composition of the Ti 6Al 2Nb 1Ta 1Mo (Ti)

Ti	Al	Nb	Ta	Mo	Fe	O	C	N	H	Ti
wt%	5.95	2.12	1.16	1.05	0.16	0.08	0.02	0.02	0.01	bal.

received in plate form with a thickness of 10 mm; chemical composition is given in Table 1 and 2. Samples of 20 × 10 × 2 mm were cut from the two alloys for the electrochemical test and microstructure observation and sealed in a mixture of epoxy resins with an exposed surface of 2 cm^2.

The electrochemical methods were used for Pitting and Crevice Corrosion Resistance of specimens alloys by using different concentrations of sodium chloride and a mix of sodium chloride and magnesium chloride solutions. Solutions with different percentages varying the chloride concentration with the presence of MgCl$_2$ and acidity (pH) of the solution were used. Tables 2 and 3 show the electrochemical corrosion parameters of DSS and Ti alloys, including test temperatures, the types of solutions, pH, and chloride concentrations of the solution. The samples were prepared from the two alloys by connecting a copper wire to one face of the sample; The samples with wire attached were then cold mounted in resin and dried in air for 24 hours at room temperature. The samples were consecutively wet grinded with 1200, 2400, and 4000 SiC paper and then polished sequentially using 6, 3, and 1 lm diamond paste. The samples were cleaned ultrasonically in an acetone bath and dried in a cool airflow before the electrochemical measurements. The surface morphology of samples was identified by scanning electron microscopy (SEM) "HITACHI X-50" to assess the pitting and crevices corrosion behavior.

2.2 Potentiodynamic polarization technique

Electrochemical measurements were performed in a bottom-up circular polarizing cell using a VersaSTAT3 potentiostat from Princeton Applied Research linked to a computer. A standard three-electrode cell was used, the counter electrode was a platinum plate, and all potential values were reported for the saturated calomel electrode (SCE). Haber Luggin capillary was put close to the working electrode. The test was done under three different temperatures, 54 ºC, 70 ºC, and 90 ºC, by using a heating jacket. These temperatures were selected due to their common applications with duplex steels and titanium alloys. All the potentiodynamic polarization experiments were performed after the stabilization of the free corrosion potential. The scan rate used was 1 mV/s. The corrosion was determined using the Tafel extrapolation method. The Corrosion rate (in mpy), which was taken from the extrapolation of the Tafel lines of each polarization curve, was estimated by the following equation:

$$C.R. = \frac{I_{corr} \times K \times EW}{\rho \times A}$$

Where I_{corr} = corrosion current density in Ampere (A), K = constant that defines the units of corrosion rate (1.288 × 105 mils/A cm year), EW = equivalent weight in (g/equivalent), ρ = density and A = sample area in cm^2. The equation indicates that, corrosion rate is directly proportional to corrosion current density.

2.3 Electrochemical impedance spectroscopy technique

Electrochemical impedance spectroscopy (EIS) is a strong technique that uses a small amplitude, alternating current (AC) signal to investigate the impedance properties of a cell. The AC signal is scanned over a broad range of frequencies to produce an impedance spectrum for the electrochemical cell under test. All electrochemical impedance spectroscopy (EIS) were performed at the same three-electrode cell arrangement as potentiodynamic polarization curves. To reach a steady state, every sample was held at least for 20 minutes at an open circuit prior to the EIS experiments. EIS was conducted in the frequency range of 100 kHz-

100mHz, with a potential sine wave amplitude of 10mV (rms). The impedance diagrams are given in the Nyquist plots representation.

3. Results and Discussion

A wide range of corrosive solution parameters were selected to increase the knowledge about the corrosion behaviour in many environments in that these alloys can serve. In this section, we will consider the effect of changing the concentration of sodium chloride and then investigate the effect of pH and temperature with the presence of $MgCl_2$ ions on the corrosion performance of DSS and Ti alloys.

3.1 Effect of sodium chloride concentration

The results obtained from the potentiodynamic polarization test are given in Table 3 and Fig. 1. It notices that increasing the concentration of sodium chloride had an essential effect on increasing the corrosion current density and then the corrosion rate of the DSS alloy at 90 °C and pH 7. While there was no significant effect on the corrosion behavior of Ti alloy under the same conditions as shown in Table 4 and Fig. 2. This claim is corroborated by the SEM examination shown in Fig. 3, which shows the presence of several pits and crevices on the surface of DSS specimens, which gradually increased with increasing NaCl concentration. While Fig. 4 shows the absence of these defects on the surface of the Ti

Table 3. Results of potentiodynamic polarization of DSS alloy at different conditions

Conditions	pH	Temp. °C	Current density, i_{corr} / μA/cm^{-2}	Potential E_{corr} / mV	Corrosion rate/ mpy
10%NaCl+3% $MgCl_2$	7.0	90	4.34	-245	1.232
10%NaCl+3% $MgCl_2$	7.0	70	1.75	-248	0.502
10%NaCl+3% $MgCl_2$	7.0	54	1.50	-266	0.411
20%NaCl	7.0	90	8.03	-315	1.968
10%NaCl	7.0	90	3.78	-303	1.037
5%NaCl	7.0	90	2.13	-261	0.712
10%NaCl+3% $MgCl_2$	4.0	90	5.10	-732	1.390
10%NaCl+3% $MgCl_2$	2.0	90	27.31	-445	8.24
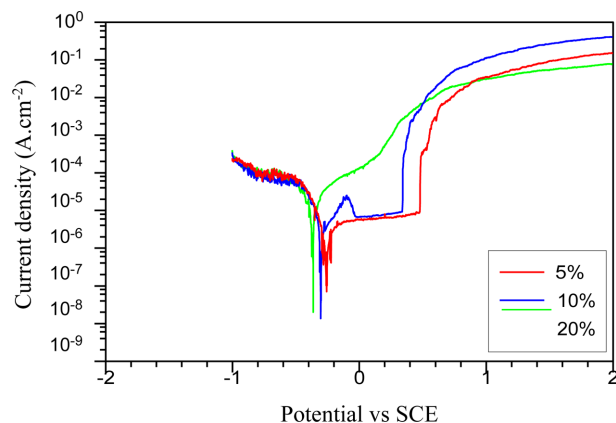
Fig. 1. the effect of chloride concentration on the corrosion resistance of DSS alloy at 90 °C and pH7
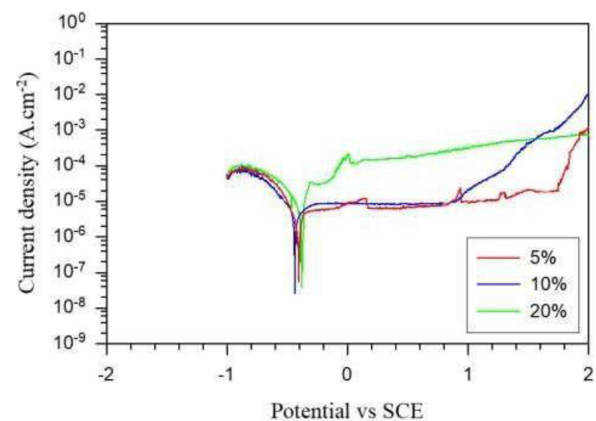
Fig. 2. the effect of chloride concentration on the corrosion resistance of Ti alloy at 90 °C and pH7
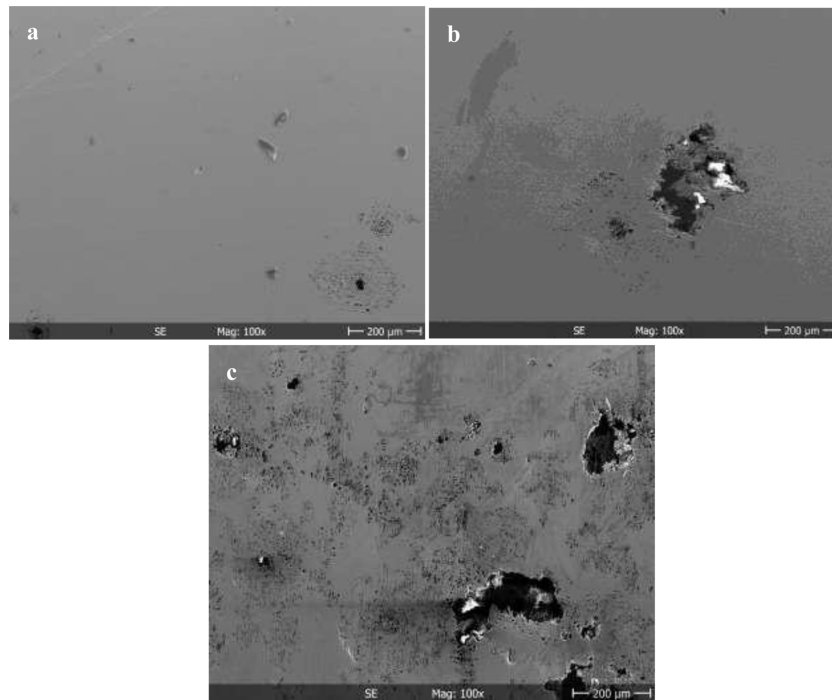
Fig. 3. SEM of DSS alloy at 90 ^{o}C, pH7 and concentrations: (a) 5% , (b) 10% and (c) 20%
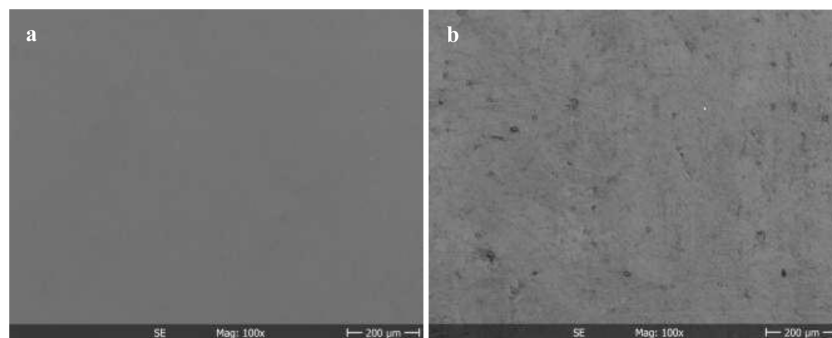

Fig. 4. SEM of Ti alloy at 90 ^{o}C, pH7 and concentrations: (a) 5% and (b) 20%

samples that were examined under identical conditions. The corrosion behaviour can be further investigated using electrochemical impedance spectroscopy (EIS). Figs. 5 and 6 show Nyquist plots obtained in a solution of various sodium chloride concentrations. Nyquist plots are often employed in the electrochemical literature because they permit for a straightforward prognosis of the circuit elements [15,16]. The Nyquist curve is a plot of real(Z/) against imaginary impedance (Z//). The bigger the radii of arc are, the higher the electrochemical impedance will be. This test supports the results obtained in the electrochemical polarization, where we notice a significant decrease in the electrochemical impedance
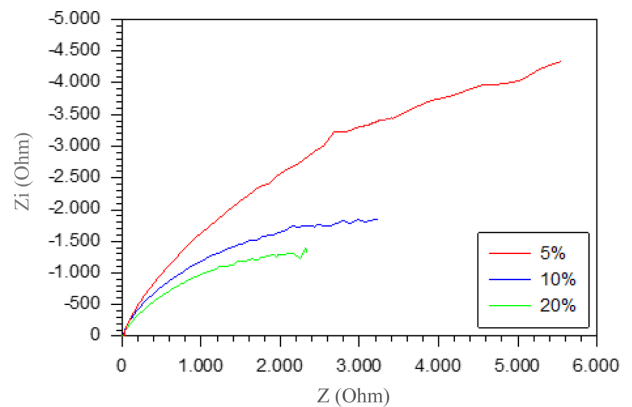

Fig. 5. Nyquist plots of chloride concentration effect on the corrosion impedance of DSS alloy at 90 ^{o}C and pH7
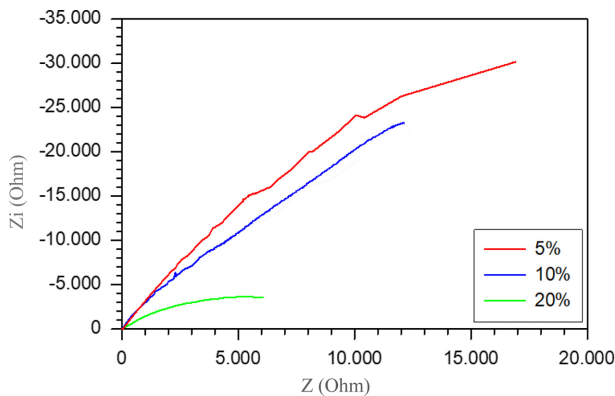
Fig. 6. Nyquist plots of chloride concentration effect on the corrosion impedance of Ti alloy at 90 °C and pH7

Fig. 7. potentiodynamic polarization of different pH effect of 10%Nacl+3%MgCl$_2$ solution on the corrosion resistance of DSS at 90 °C

Fig. 8. potentiodynamic polarization of different pH effect of 10%Nacl+3%MgCl$_2$ solution on the corrosion resistance of Ti at 90 °C

of both alloys with the increase in the concentration of sodium chloride.

The increase of chloride ions incorporates a noteworthy effect on the corrosion behaviour of DSS; since the presence of these ions, a passivity breakdown process takes place above a certain potential that decreases with the chloride concentration. Chloride ions bit by bit penetrate into the surface, at which the protective film is destroyed, and the steel begins to corrode. Chloride corrosion tends to pit the entire surface area of the samples evenly with shallow, irregularly shaped pits. The penetration of chloride into the metal is due to the presence of various mechanisms, the most important of which are diffusion and capillary absorption [17]. The effect of increasing the concentrations of sodium chloride on the corrosion resistance of Ti alloy was slight compared to that of DSS alloy, mainly due to the fact that the Ti alloy contains Mo elements, which makes the passive film more stable [18]. In addition, it is reported that Al could be oxidized and form a compact Al oxide layer on the top of the passive film, inhibiting the dissolution of the oxide film [19].

3.2 Effect of acidity (pH)

It was reported in a previous study [20] that the corrosion in the magnesium chloride solution is higher than the sodium chloride due to the relatively high viscosity compared to the sodium chloride solution. Because of multiple operating environments and to cover the maximum possible of the influencing surrounding environment factors, it is necessary to study the effect
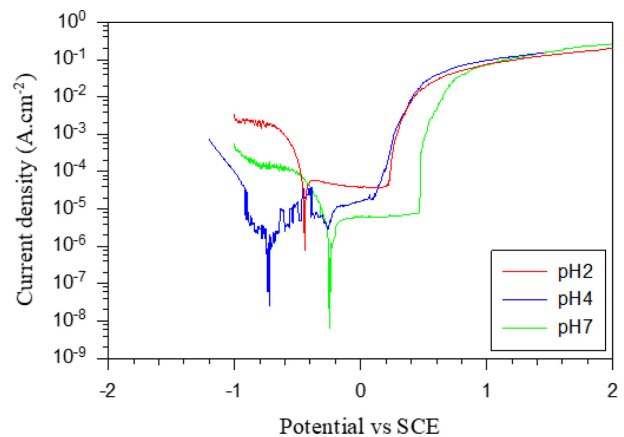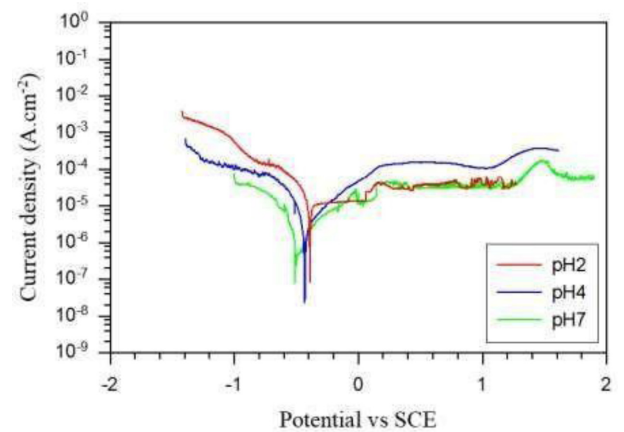
of a mixture of these two solutions on the corrosion performance under relatively high temperatures and multiple pH values. The samples were tested in 10% sodium chloride solution with 3% magnesium chloride added at pH 7, 4, and 2 at 90 °C.

Fig. 7 and Table 3 show the potentiodynamic polarization curve and the data deduced from this curve. We note that the pH decrease led to a significant reduction in the corrosion resistance of the DSS alloy. Where the data in Table 3 showed an excessive increase in the corrosion current density and the corrosion rate from 4.34 μA/cm^{-2}, 1.23 mpy to 27.31 μA/cm^{-2}, and 8.24 mpy when decreasing the pH from 7 to 2, respectively.

Likewise, titanium alloy shows a noticeable increase of the corrosion current density from 3.6 μA/cm^{-2} to

Table 4. Results of potentiodynamic polarization of Ti alloy at different conditions

Conditions	pH	Temp. °C	Current density, i_{corr}/μA/cm^{-2}	Potential E_{corr}/ mV	Corrosion rate/mpy
10%NaCl+3% MgCl$_2$	7.0	90	3.06	-461	0.695
10%NaCl+3% MgCl$_2$	7.0	70	0.827	4-78	0.185
10%NaCl+3% MgCl$_2$	7.0	54	0.477	-408	0.107
20%NaCl	7.0	90	2.92	-431	0.659
10%NaCl	7.0	90	2.87	-442	0.648
5%NaCl	7.0	90	2.78	-405	0.628
10%NaCl+3% MgCl$_2$	4.0	90	3.69	-431	0.816
10%NaCl+3% MgCl$_2$	2.0	90	4.24	-386	0.958
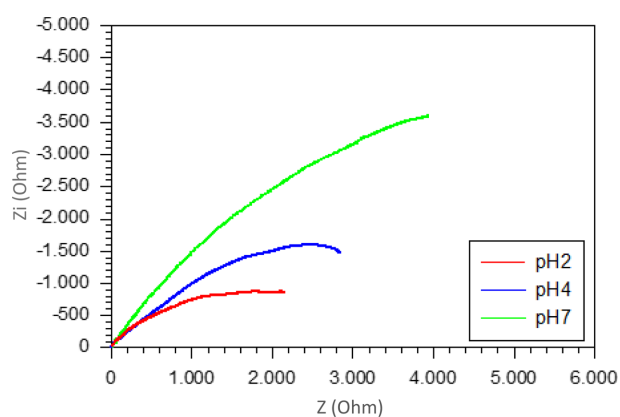
Fig. 9. Nyquist plots of different pH effect of 10%Nacl +3%MgCl$_2$ solution on the corrosion impedance of DSS at 90 °C
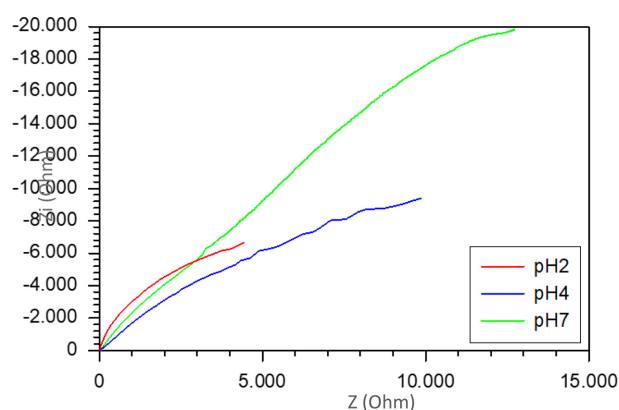
Fig. 10. Nyquist plots of different pH effect of 10%Nacl +3%MgCl$_2$ solution on the corrosion impedance of Ti at 90 °C

4.24 μA/cm^{-2} and the corrosion rate from 0.695 mpy to 0.958 mpy with the decrease in the pH from 7 to 2, respectively, as shown in Fig. 8 and Table 4.

Further investigations were necessary to re-verify the significant increase in the corrosion rate, and to remove doubt, especially for the DSS alloy with pH reduction. EIS results proved a considerable decrease in the corrosion resistance again. Fig. 9 shows the drop in impedance from 3.91 kΩ to 1.41 kΩ with pH decreasing from 7 to 2 for DSS alloys. Fig. 10 also shows a decrease in the impedance of Ti alloy with reducing the acidity of the solution. The impedance decreased from 23.51 kΩ to 13.16 kΩ, then to 8.01 kΩ, with pH decreasing from 7 to 4 and 2, respectively.

The metallographic observations shore the results obtained from the electrochemical investigations where SEM and optical microscopy showed the increased pitting and their size in the surface of DSS alloy with pH decreasing, as shown in Figs 11 and 12. While the Ti alloy showed crevices on the surface of the samples tested in solution at pH 2, and it didn't appear at pH 7 and 4.

The addition of magnesium chloride played an important factor in increasing the corrosion rates of the two alloys, which is consistent with what was stated in the previous study [20]. It found that the increase in corrosion rate was due to the MgCl$_2$ solution having a higher viscosity and stronger hydrophilicity than the NaCl solution, which makes the MgCl$_2$ particles stick and crystallize on the
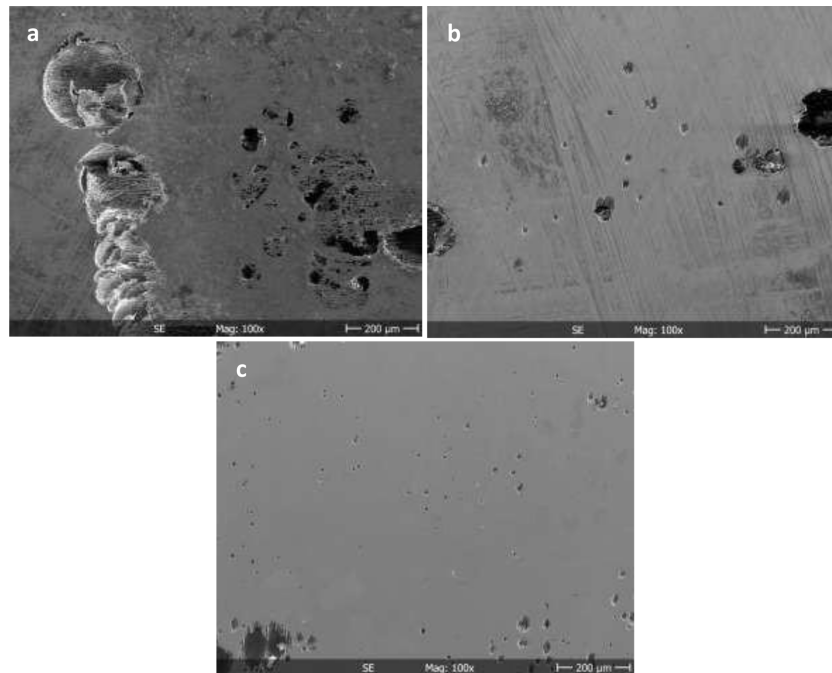
Fig. 11. SEM of DSS tested in 10%Nacl+3%MgCl$_2$ solution at 90 ^{o}C and pH: (a) 2 , (b) 4 and (c) 7
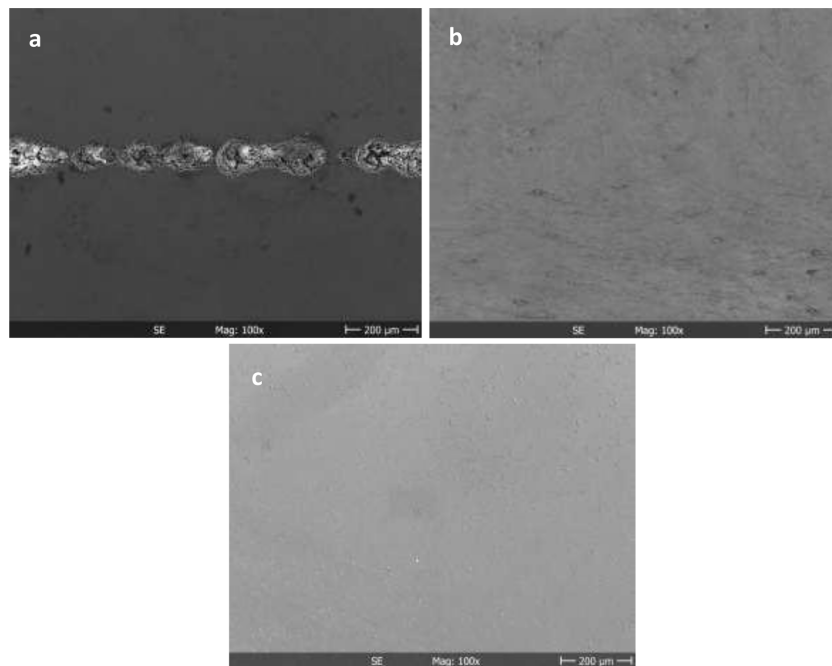

Fig. 12. SEM of Ti tested in 10%Nacl+3%MgCl$_2$ solution at 90 ^{o}C and pH: (a) 2 , (b) 4 and (c)7

surface and react with metal quickly.

Generally, corrosion resistance of stainless steels is achieved by dissolving sufficient chromium in iron to produce a coherent, adherent, insulating, and regenerating chromium oxide protective layer (Cr$_2$O$_3$) on the surface.

This passive film of chromium oxide formed in the air at room temperature is only about 1–2 nm. Pitting corrosion results from the local destruction of the passive film and subsequent corrosion of the steel underneath this layer. The DSS micrographs in Fig. 7 showed that

the pit evolution frequency increased with the pH reduction because low pH solutions accelerate corrosion by providing hydrogen ions. Hydrogen attacks and damages the surface of steel and increases the rate of corrosion [21]. The pits formation is influenced by many factors, such as the presence of a highly corrosive film containing chloride compounds because negatively charged chloride ions migrate into the pit to balance the positively charged metal ions. Previous studies reported that the equilibrium ferrite/austenite structures could promote galvanic corrosion with the dissolution of ferrite in open circuit conditions [22,23].

Appearing the crevices on the surface of Ti alloy at pH 2, as shown in Fig. 8, was due to the dissolve oxide film of Ti. It was reported that strong reducing acidity dissolves the Ti oxide film easily, and the alloy is activated and prone to attack. If the acidity is strong enough, a Ti hydride film is formed on the surface of Ti once the oxide film has been dissolved. The Ti hydride film is equally protective, but it does not grow spontaneously like anatase and rutile [24].

3.3. Effect of temperature

The electrochemical corrosion tests shown in Fig. 13 and Table 3 indicate the corrosion rate and current density of the DSS alloy at 54 °C are much lower compared to the samples tested at 90 °C. Nyquist plot of DSS (Fig. 14) shows a significant increase in impedance from 3.91 kΩ at 90 °C to 8.95 kΩ at 54 °C. The same applies to Ti alloy, where the decrease in temperature reduced the corrosion rate and corrosion current density from 0.695 mpy/ 3.06 μA/cm^{-2} at temperature 90 °C to 0.107 mpy/ 0.477 μA/cm^{-2} at temperature 54 °C, as shown in Fig. 15. SEM observations in Fig. 16 of DDS alloy tested at 54 °C show very small and few pits compared with the samples tested at 90 °C, which showed increased number and size on the surface. In contrast, SEM of the Ti alloy shown in Fig. 17 indicated a clean surface and was unaffected by the corrosion test at all temperatures. The results deduced from the electrochemical experiments and metallographic observations confirmed that temperature plays a crucial role in influencing corrosion resistance. The high corrosion rate of DSS may be related to the high dissolution and instability of oxide film at 90 °C.
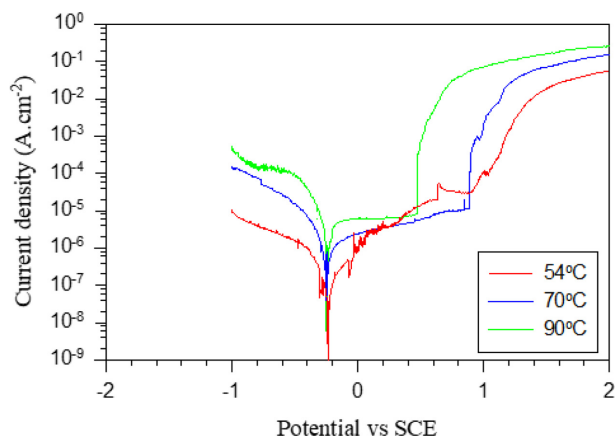

Fig. 13. potentiodynamic polarization of the temperature effect on the corrosion resistance of DSS in 10%Nacl +3%MgCl$_2$ solution and pH7
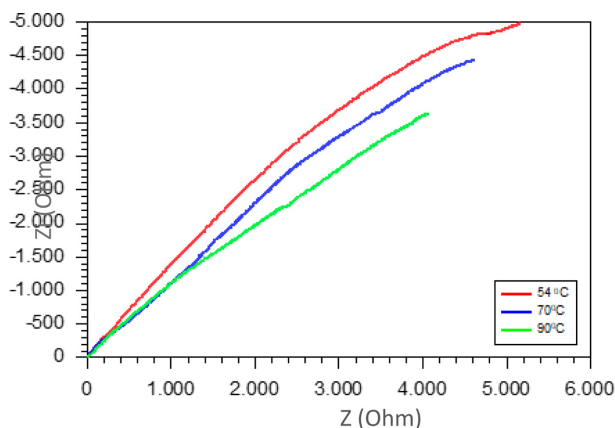

Fig. 14. Nyquist plots of the temperature effect on the corrosion impedance of DSS in 10%Nacl+3%MgCl$_2$ solution and pH7

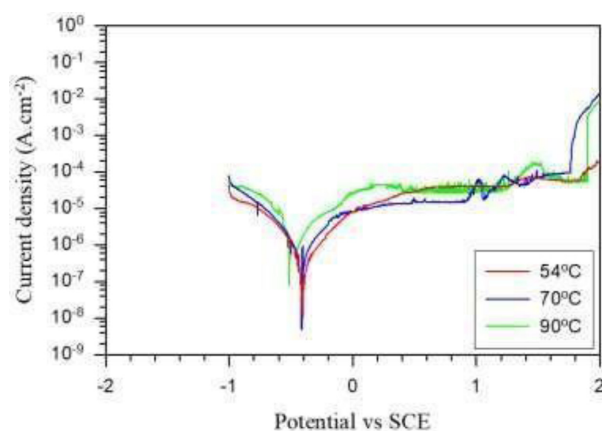**Fig. 15. potentiodynamic polarization of the temperature effect on the corrosion resistance of Ti alloy in 10%Nacl +3%MgCl$_2$ solution and pH 7**
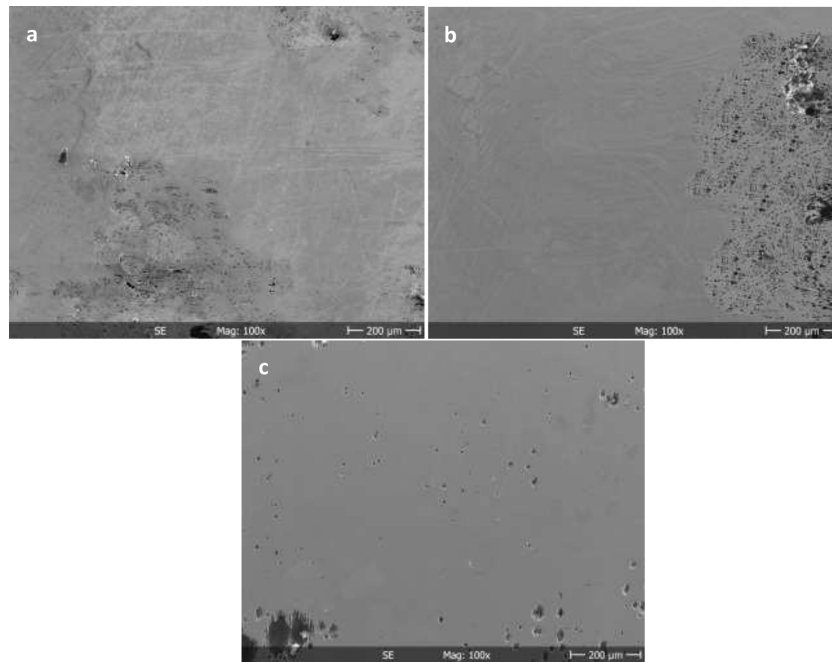
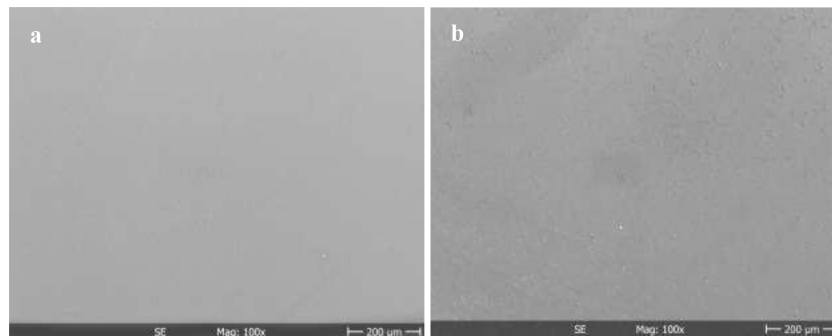**Fig. 16. SEM of DSS tested in 10%Nacl+3%MgCl$_2$ pH7 solution at: (a) 54 $^{\circ}$C , (b) 70 $^{\circ}$C and (c) 90 $^{\circ}$C**

Fig. 17. SEM of Ti tested in 10%Nacl+3%MgCl$_2$ pH7 solution at: (a) 54 $^{\circ}$C , and (b) 90 $^{\circ}$C

This is in good agreement with the previous study [25]. It was found that the increased temperature from 25-80 $^{\circ}$C increases the corrosion rates, the current density of duplex stainless steel in 1 M sulphuric acid contaminated with 1% NaCl.

Jing Liu et al. [26] studied the effects of temperature (100 - 230 $^{\circ}$C) and sulphate concentration on the Pitting Corrosion of Titanium. He considered the temperature and sulphate ions are two critical parameters in the pitting corrosion of Ti. Furthermore, it was noted that the dimension of the pits increased as the operating temperature increased, While no pit formation was observed at 100 $^{\circ}$C. Another study [27] investigated the corrosion behaviour of five titanium alloys in artificial seawater over the temperature range of 25 $^{\circ}$C to 200 $^{\circ}$C. It found that all five grades of titanium resist cracking and pitting corrosion under 80 $^{\circ}$C, while only the commercial titanium grades suffer from crevices corrosion in the range of temperature between 80 $^{\circ}$C and 200 $^{\circ}$C.

The results obtained from electrochemical corrosion tests and microscopic examination proved that Ti alloys have superiority over DSS alloys regards corrosion and pitting resistance under all conditions. This is due to several factors, such as the elements that make up the alloy, like Al, Mo, and Ta, which make the oxide film more stable. In addition, the reason for the predominance of Ti alloy over DSS in terms the corrosion resistance is mainly because the base element in the alloy is

titanium, which forms titanium oxide, the peer of chromium oxide in protecting the base alloy. At the same time, DSS can be the ideal alternative to Ti alloys because of its excellent corrosion resistance compared to conventional stainless steel and its lower cost compared to titanium alloys.

4. Conclusions

The current study aimed to differentiate between duplex stainless steel and Ti alloys regards their corrosion performance in complicated environmental variables, including fluctuations in chloride concentrations, adding magnesium ions, differences in pH, and relatively high temperatures. The main conclusions that can draw from this study are:

1. The Ti alloy has superiority over duplex stainless steel alloy regarding the corrosion resistance at all conditions.

2. Led pH reduction to significantly increase the current density and corrosion rate of both alloys.

3. The increase in the chloride concentration and temperature had a more substantial impact on the corrosion behavior of DSS than on Ti alloys.

4. The pitting corrosion was formed on the DSS samples in all conditions, while the crevice corrosion was developed on the Ti samples with the presence of magnesium chloride at pH 2 and 90 °C.

5. Magnesium chloride ions in a low acidity solution appear to interact with the re-passivation at the surface of these alloys and influence the resulting surface topography.

References

1. Stephen J. Morrow, Materials Selection For Seawater Pumps, Turbomachinery Laboratory, Texas A&M University (2010). Doi: https://doi.org/10.21423/R10G9H

2. Pharic Smith, Thomas Kraenzler, Maximizing Pump Efficiency through Reduced Corrosion and Erosion, Empowering Pumps and Equipment, January 16 (2017). https://empoweringpumps.com/sulzer-maximizing-pump-efficiency-through-reduced-corrosion-erosion/

3. F. Gall, *Proc. Pumps and Compressors Conf.*, Session 9, pp. 1 – 29, Perth, Australia (2013). https://www.idc-online.com/conferences/1306FrankPaper.pdf

4. R.W. Shutz, D.E. Thomas, ASM Metals Handbook, Corrosion, *vol. 13, ninth ed.*, p. 669, ASM International, Metals Park, OH (1987).

5. T. Ohtsuka, M. Masuda, and N. Sato, Ellipsometric Study of Anodic Oxide Films on Titanium in Hydrochloric Acid, Sulfuric Acid, and Phosphate Solution, *Journal of The Electrochemical Society,* **132**, 787 (1985). Doi: https://doi.org/10.1149/1.2113958

6. T. M. Yue, J. K. Yu, Z. Mei, H. C. Man, Excimer laser surface treatment of Ti–6Al–4V alloy for corrosion resistance enhancement, *Materials Letters*, **52**, 206 (2002). Doi: https://doi.org/10.1016/S0167-577X(01)00395-0

7. C. Blanco-Pinzon, Z. Liu, K. Voisey, F. A. Bonilla, P. Skeldon, G. E. Thompson, J. Piekoszewski, A. G. Chmielewski, Excimer laser surface alloying of titanium with nickel and palladium for increased corrosion resistance, *Corrosion Science*, **47**, 1251 (2005). Doi: https://doi.org/10.1016/j.corsci.2004.06.030

8. Z. B. Wang, H. X. Hu, Y. G. Zheng, W. Ke, Y. X. Qiao, Comparison of the corrosion behavior of pure titanium and its alloys in fluoride-containing sulfuric acid, *Corrosion Science*, **103**, 50 (2016). Doi: https://doi.org/10.1016/j.corsci.2015.11.003

9. R. C. Newman, The dissolution and passivation kinetics of stainless alloys containing molybdenum- I. Coulometric studies of Fe-Cr and Fe-Cr-Mo alloys, *Corrosion Science*, **25**, 331 (1985). Doi: https://doi.org/10.1016/0010-938X(85)90111-8

10. P. Marcus, On some fundamental factors in the effect of alloying elements on passivation of alloys, *Corrosion Science*, **36**, 2155 (1994). Doi: https://doi.org/10.1016/0010-938X(94)90013-2

11. C. Ouchi, H. Fukai, K. Hasegawa, Microstructural characteristics and unique properties obtained by solution treating or aging in β-rich α+β titanium alloy, *Materials Science and Engineering A*, **263**, 132 (1999). Doi: https://doi.org/10.1016/S0921-5093(98)01171-X

12. Erween Abd Rahim, S. Safian, Investigation on tool life

and surface integrity when drilling Ti- 6Al-4V and Ti-5Al-4V-Mo/Fe, *JSME International Journal Series C*, **49**, 340 (2006). Doi: https://doi.org/10.1299/jsmec.49.340

13. J. Charles, Super Duplex Stainless Steels: Structure and Properties, *Proc. Duplex Stainless Steels '91 Conf.*, pp. 151 – 168, Les Editions de Physique, Vol. 1, Les Ulis Cedex, France (1991).

14. D. S. Bergstrom, J. J. Dunn, J. F. Grubb, and W. A. Pratt, US20036551420B1 (2003).

15. B. Wei, J.C. Tokash, F. Zhang, Y. Kim, B.E. Logan, Electrochemical analysis of separators used in single-chamber, air–cathode microbial fuel cells, Electrochimica Acta,, **89**, 45 (2013). Doi: https://doi.org/10.1016/j.electacta.2012.11.004

16. X. G. Han, F. Zhu, X. P. Zhu, M. K. Lei, J. J. Xu, Electrochemical corrosion behavior of modified MAO film on magnesium alloy AZ31 irradiated by high intensity pulsed ion beam, *Surface and Coatings Technology*, **228**, S164 (2013). Doi: https://doi.org/10.1016/j.surfcoat.2012.06.053

17. Yunan Prawoto, Khaled M. Ibrahim, wan sani wan nik, Effect of ph and chloride concentration on the corrosion of duplex stainless steel, *Arabian Journal for Science and Engineering*, **34**, 2 (2009).

18. B. J. Wang, D. K. Xu, S. D. Wang, E. H. Han, Fatigue crack initiation of Magnesium alloys under elastic stress amplitudes: A review, *Frontiers of Mechanical Engineering,*, **14**, 113 (2019). Doi: https://doi.org/10.1007/s11465-018-0482-1

19. J. W. Lu, Y. Q. Zhao, H. Z. Niu, Y. S. Zhang, Y. Z. Du, W. Zhang, W. T. Huo, Electrochemical corrosion behavior and elasticity properties of Ti-6Al-xFe alloys for biomedical applications, *Materials Science and Engineering C*, **62**, 36 (2016). Doi: https://doi.org/10.1016/j.msec.2016.01.019

20. Xi Yunping, Xie Zhaohui, Corrosion Effects of Magnesium Chloride and Sodium Chloride on Automobile Components, Report No. CDOT-DTD-R-2002-4. https://www.codot.gov/programs/research/pdfs/2002/magautocor.pdf

21. In Hyoung Rhee, Hyunjun Jung, Daechul Cho, Evaluation of pH control agents influencing on corrosion of carbon steel in secondary water chemistry condition of pressurized water reactor, *Nuclear Engineering and Technology*, **46**, 431, (2014). Doi: https://doi.org/10.5516/NET.09.2013.076

22. E. Symniotis, Galvanic effects on the active dissolution of duplex stainless steels, *Corrosion*, **46**, 2 (1990). Doi: https://doi.org/10.5006/1.3585062

23. Y.-H. Yau, M. A. Streicher, Galvanic corrosion of duplex FeCr-10% Ni alloys in reducing acids, *Corrosion*, **43**, 366 (1987). Doi: https://doi.org/10.5006/1.3583872

24. Michael O. Bodunrin, Lesley H. Chown, Josias W. van der Merwe, Kenneth K. Alaneme, Christian Oganbule, Desmond E.P. Klenam und Nthape P. Mphasha, Corrosion behavior of titanium alloys in acidic and saline media: role of alloy design, passivation integrity, and electrolyte modification, *Corrosion Reviews*, **38**, 25 (2020). Doi: https://doi.org/10.1515/corrrev-2019-0029

25. Oluwatoyin Adenike Olaseinde, Comparative Study of the Effect of Temperature on the Corrosion Behaviour of 2205 Duplex Stainless Steel and 316 Stainless Steel in Acidic Chloride Environment, *Advances in Materials Physics and Chemistry*, **5**,185 (2015). Doi: https://doi.org/10.4236/ampc.2015.55019

26. Jing Liu, Akram Alfantazi, Edouard Asselin, Effects of Temperature and Sulfate on the Pitting Corrosion of Titanium in High-Temperature Chloride Solutions, *Journal of The Electrochemical Society*, **162**, C189 (2015). Doi: https://doi.org/10.1149/2.0541504jes

27. Jianjun Pang, Daniel J Blackwood, Corrosion of Titanium Alloys in High Temperature Seawater, *Corrosion Science and Technology*, **14**, 195 (2015). Doi: https://doi.org/10.14773/cst.2015.14.4.195